

Design and Implementation of Different Unit Cells for Reconfigurable Intelligent Surface

Jaafar Qassim Kadhim^{1*}, Adheed H. Sallomi², Iryna Svyd³

^{1,2} Electrical Engineering Department, College of Engineering, Mustansiriya University, Baghdad, Iraq

³ Kharkiv National University of Radio Electronics, Kharkiv

¹<https://orcid.org/0000-0002-8193-2314>,

²<https://orcid.org/0000-0001-5972-2612>

³<https://orcid.org/0000-0002-4635-6542>

*Email: jaafar80@uomustansiriyah.edu.iq

Article Info

Received 06/11/2023

Revised 24/04/2024

Accepted 07/06/2024

Abstract

Recently, great attention has been given to the idea of a smart environment. It often involves the use of reconfigurable intelligent surfaces (RIS) for the management of electromagnetic wave reflections as the world awaits the emergence of 6G. Changeable intelligent surfaces may enhance the creation of wireless communication. The design and analysis of several unit cell reflections are presented in this work. The first design relies on the Switching Technique which involves switching on and off to acquire the phase as well as the coefficient of reflection to accommodate 6G standards. The unit cells design is configured to operate in the millimeter band and X band. In the second design, the radius of the circular patch was changed to adjustment of the phase and reflection coefficient. The use of Floquet technique is employed in investigating the scattering characteristics of a unit cell's constituent elements based on the assumption that every element consists of an extremely iterating periodic structure. To determine the optimal force reflection and the transformation phase, the return loss alongside reflection phase graphs of each resonant component were examined. The simulation results indicate that the first design exhibits a reflection phase shift range of -180 to 90 and a reflection magnitude over 0.93 at a frequency of 11GHz. In contrast, the second design demonstrates a reflection phase shift range of -135 to 135 and a reflection magnitude surpassing 0.9 at a frequency of 28GHz. The analysis and simulation of the design models were carried out using the CST model.

Keywords: Floquet technique; Reconfigurable Intelligent Surfaces; Smart environments; Switch configurations

1. Introduction

The idea of smart environments was presented in [1]-[2], where the researcher suggested controlling the electromagnetic reflectiveness of a building's walls to optimize the distribution of the signal inside the building in accordance with requirements. A little later, in [3]-[4], electronically reconfigurable surfaces were proposed as a way to improve wireless communications. In these papers, the surface's fields were locally manipulated to concentrate on a certain antenna. Consequently, the concept of smart environments using electronically changeable surfaces, known as changeable Intelligent Surfaces (RIS), appeared as a significant improvement for 6G and it has since gained a huge and expanding amount of interest in the wireless communications world. Numerous research topics are connected to RIS, such as wavefront shaping with RIS [5]-[7], stochastic analysis

approach [8]-[9], RIS-based signal modulation and the encoding [10]-[11], MIMO channel was estimated and beamformed [12]-[14], evaluation of the telecommunication performance [15], and the energy-efficient wireless communication [16]-[17]. However, a significant portion of the many publications that have been suggested are focused on theoretical and mathematical methods, and relatively few of them deal with experimental proofs of RIS. RIS consists of a number of unit cells, and each one of the unit cells is able to tune the phase or magnitude of the reflected wave. The reconfigurable intelligent surfaces (RIS) can be affixed to the exterior surface of various architectural structures. Moreover, these devices exhibit advantageous characteristics such as cost-effectiveness and low energy consumption. Therefore, the utilization of RIS can lead to a substantial enhancement in communication performance. Many of the suggested papers focus on theoretical and mathematical methodologies and deal

less with experimental evidence of RIS. Each one of the unit cells in RIS is able to tune the phase or magnitude of the reflected wave. This paper discusses the use of a multi-method strategy for adjusting the phase difference and magnitude. This provides a better knowledge of how a unit cell is identified in the design of reconfigurable intelligent surfaces. In addition, switching and variable length approaches were employed to produce the necessary phase and reflection coefficients.

1.1. Concepts and Developments of RIS

As soon as it was developed, RIS caught the interest of both academics and industry due to its flexibility in modifying the electromagnetic properties of wireless channels, as seen in Fig. 1. The development of a smart radio environment is made possible by RIS introduction, which allows the environment of the wireless propagation, which passively could only be adjusted previously, to now be controlled. Being a two-dimensional application of metamaterials, RIS possesses the qualities of affordability in a natural manner, simplicity, and deployment ease. It could help wireless networks meet upcoming needs and overcome challenges [18]- [19].

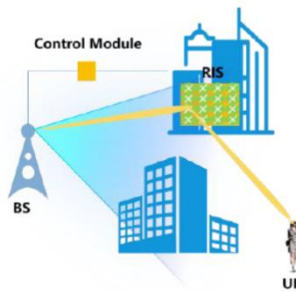


Figure 1. Reconfigurable Intelligent Surfaces conceptual illustration

RIS has a propensity to emerge as a major breakthrough technology. In order to satisfy the demands of future mobile communication, RIS's promise lies in its ability to be used with 5G-Advanced as well as in the ability to create a new communication network paradigm in 6G [20]-[21]. The domestic industrial circles also conducted a number of RIS tests and verifications in the present network. Results show that RIS adoption can significantly increase wireless networks' throughput and coverage. RIS has shown strong performance in a number of domains as a technique for dynamically adjustable electromagnetic characteristics [22]. Before being implemented on a broad scale in the commercial sector, RIS still has a lot of issues and hurdles to overcome in the areas of technological research, engineering application, network deployment, and standardization.

1.2. Principle Operation of RIS

The designing of RIS can be done through the use of patch types of unit cells metamaterial-based unit cells, or even any

other kind of method [23]-[24]. Also, it is possible to reconfigure the waves that are transmitted or reflected by the RIS. In addition, the RIS may exhibit refractive incident waves. Fundamentally, every RIS is made up of several unit cells which can be tuned in a manner that allows them to have impedance. The illustration of a typical electric conductor that possesses the same impedance upon the surface (η_s) is presented in Fig. 2. Therefore, in the case of a perfect conductor, the angle of incoming waves and reflected waves are equal. This means that there is no difference between the two angles. Nevertheless, in the case of RIS, there can be variation in the surface impedances from one point to another as seen in Fig.3. The varying surface impedances for the RIS in Fig. 3 are η_{s1} , η_{s2} , η_{s3} , η_{s4} , η_{s5} , η_{s6} , and η_{s7} . Due to the differences in the surfaces' impedances, changes occur in the reflected waves. The continuous variation of the RIS' surface impedance at a specific RIS location can result in dynamic phase variation. Thus, a variation that occurs on the RIS' surface causes the occurrence of constructive interference in the desired direction. Also, when the RIS surface impedance is changed, constructive interference will occur in various directions. Thus, by varying the surface impedance, an RIS can be achieved. There is a relationship between the reflection coefficient and the impedance of the surface, which is represented by [25]

$$\Gamma = (\eta_s - \eta_0)/(\eta_s + \eta_0) \quad (1)$$

where Γ represents the coefficient of reflection, η_s denotes the impedance of the surface, and η_0 is the impedance of the free space wave. The transmission coefficient can be expressed as follows:

$$1 + \Gamma = (2\eta_s)/(\eta_s + \eta_0) \quad (2)$$

The validity of Equ. (1) and Equ. (2) is confirmed in the area with the same surface impedance. The following expression denotes the reflection coefficient of the RIS

$$\Gamma_n = (\eta_{sn} - \eta_0)/(\eta_{sn} + \eta_0) \quad (3)$$

where $n=1,2,3,4,5,6$, and 7 . η_{sn} represents the surface impedance for various areas of the surface. This means that the various regions of RIS have varying coefficients of reflection.

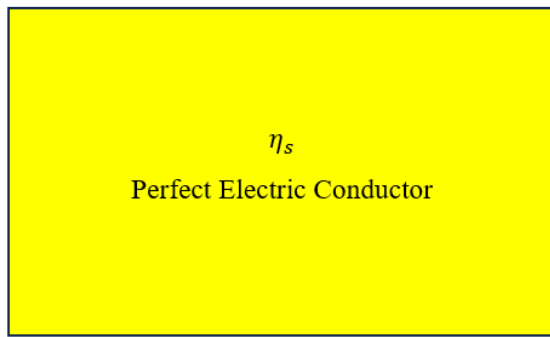


Figure 2. Identical surface impedance in a perfect electrical conductor

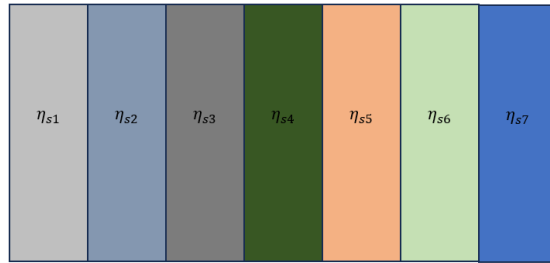


Figure 3. RIS with various surface impedances

1.3. Unit cells Switch Configurations

A unit cell is a type of planar microstructure that is a basic component of RIS. Rectangular arrays of unit cells are arranged to attain a flat surface. The unit cell's size depends on the operating frequency; smaller dimensions are needed at higher frequencies. A fixed-size RIS's size and shape determine how many unit cells it contains overall. Large RIS can be created by connecting several smaller surfaces with the unit-cell repeating pattern. It is expected that the resulting RIS will have flexible and real-time capability by incorporating active electrical components, including PIN diodes, into unit-cell architecture.

Switches are the most widely used method of reconfiguration. However, the most widely used switches include PIN diodes and varactors.

1.3.1 PIN Diodes

A PIN diode can be described as a packaged semiconductor device that possesses p-type, I- and n-type regions. Normally, in between the p-type and n-type regions lies a high resistivity intrinsic I region [26]. The outcome of forward biasing the PIN diode is the injection of the -I region with electrons and holes. The result of this will be an average stored charge that lasts for a lifetime. When the PIN diode is subjected to the process of reverse biasing it results in the absence of charge within the -I region with the diode appearing as a capacitor in a shunt with a resistor. An important factor to consider before subjecting the PIN diodes to the process of biasing is the need for a steady DC current for its activation. The PIN diode can be regarded as a resistor that is controlled by a current at

microwave frequencies. One of the benefits that can be derived from PIN diodes is the speed with which they switch. In other words, their switching mechanism is faster. Several authors have proposed different kinds of reconfigurable antennas that make use of PIN diodes as switches. For instance, in the work done by [27] PIN diodes were used to create a connection between four patch sections to a major patch section of a planar antenna. The authors controlled the activation of the switches using a field programmable gate array (FPGA).

1.3.2. Varactor Diode

Varactor diodes are P-N junction diodes that are characterized by changing capacitances depending on the bias that is applied. In antennas that are equipped with a varactor, the operation frequency can be tuned by tuning the varactor's capacitance. To achieve the tuning of the varactor's capacitance, it is crucial to have a different source of voltage. An RF choke must be included in the biasing lines because it helps prevent the passage of RF signals to the ground. The DC blocker is another key element that should be incorporated into the biasing lines because it helps prevent the DC signal from leaking into the structure of the antenna [28]-[29].

1.4. PIN Diode Switching Techniques

The technique for switching usually involves the use of two switches which are also regarded as pin diodes due to their ability to function like variable resistors within the radio frequency range. These PIN Diodes exhibit a behavior of the short and open circuit at the significant points of insertion, changing the length of the antenna active resonant, which in turn causes the reconfiguration of the operating frequency of the antenna. Fig.4 presents an illustration of the corresponding circuits for the OFF and ON states of a PIN Diodes switch. In one state, R and L are simply in series. When the switch is in a state of "off", it corresponds to the circuit that consists of R, L, and C, and the inductor "L" is processed in parallel form with the resistor "Rh" and the capacitor "C". In this paper, the use of a Skyworks SMP1345-079LF pin diode is employed. Also, the use of CST has been employed in simulating it as, L = 0.75 nH, C =0.18 pF, and RL =1.6 Ω based on the datasheet.

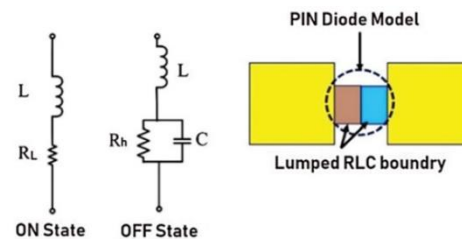


Figure 4. Pin diode equivalent circuits of the ON and OFF states.

1.5. The objective of the Work

This research primarily focuses on achieving a precise phase difference and magnitude by employing two techniques. The first technique involves creating a square patch using diodes, while the second technique involves modifying the radius of the circular patch. This approach leads to a straightforward and cost-effective design for the RIS.

2. Literature Review

In the research carried out in [30], the electromagnetic characteristics were modified by using a metal ground plane in association with a periodic surface texture. More so, the varactor diodes were incorporated within the texture to obtain an adaptable impedance surface where both the reflection phase and resonant frequency are controlled by the bias voltage. By tuning the surface, they were able to obtain a gradient of phase which produced the steered beam that reflected $\pm 40^\circ$.

In another study,[31], A sub-6 GHz band of frequencies operating varactor diode-based RIS was presented. The structure of the proposed design was equipped with 2430-unit cells and a 3.5 GHz operating frequency. The reflected beam was reconfigured using a varactor diode. Their report showed that changes made to the capacitor's capacitance resulted in the variation of the needed phase with minimal reflection loss.

Similarly, in a study by the authors in [32], a varactor diode-based RIS was designed. Their designed RIS was implemented using 1100 controllable elements operating at 5.8 GHz. To configure the RIS over air, this group of researchers proposed an efficient algorithm. 27dB a power gain was recorded within a short-distance measurement environment. In this study, the measurement of the RIS performance in an exterior setting was done at a long distance of more than 500 meters. The recorded performance of the RIS was highly satisfactory. Another group of researchers in [33] presented a RIS unit cell based on a varactor diode. According to their findings, the proposed unit cell managed to produce 277 phase shifts at 24.5 GHz with a minimal coefficient of reflection of 0.5. An mm-wave PIN diode-based RIS was presented in [34]. A comprehensive study of a PIN-based metasurface was carried out, and a broad bandwidth of about 28 GHz frequency band was obtained. Also, the unit cell was developed, and its features were verified. The last stage of their work involved the fabrication of $10\text{ cm} \times 10\text{ cm}$ of the whole RIS, as well as the verification of its performance.

In [35] a new and simple 2-bit unit cell was suggested for the realization of an RIS. Similarly, in [36] another RIS that operates at 5.8 GHz was suggested. The researchers built the unit cell using a PIN diode, a simple patch, and a 16×10 array to achieve the RIS. The unit cell was characterized by the 1-bit operating technique with the parasite patch. A

statistical analysis of the unit cells' performance was carried out by the researchers, and the results revealed that the degree of reflection between the two states was minimal with a phase difference of 180° . In another study, the authors proposed an RIS that is characterized by 2-bit high accuracy and 64 elements that can be individually controlled [37]. The authors in [38] proposed a novel kind of the 2.75-bit RIS that operated with 5G-mid-band. The proposed design had eight separate states. The unit cell presented in their study was designed with 3 PIN diodes and improved the resolution of the phase alongside lesser active component numbers. Furthermore, the algorithm of swarm optimization was used in this design to achieve the maximization of the state separation.

Similarly, a new type of a 3-bit RIS that is based on digital coding was presented in [39]. The structure proposed in this study is made up of metal patches as well as varactor diodes through which the amplitude and phase of the reflected waves can be controlled. In reference [40], the RIS utilizing the multi-bit PIN diode was introduced. This RIS is able to effectively direct the beam toward the intended direction while working within the frequency range of the sub-6 GHz. The proposed design was tested using a wide range of scenarios. The proposed RIS was built by the researchers. In the work done in [41]-[48], an RIS structure was designed using a cost-efficient FR4 substrate with 1.6 mm thickness and 4.4 permittivity parameters. The proposed RIS design, which was operated at a 3.5 GHz frequency band, was simple and cost-efficient. The researchers also covered RIS measuring methodologies and parameters.

3. Proposed Design

In this study, two models for unit cell design are proposed. The proposed design employs the use of CST software. In the first model design, the phase and reflection coefficients are obtained through the deployment of the on and off states in the switching technique. On the other hand, the second model design relies on the changes in the patch dimension to derive the phase and reflection coefficient.

Fig.5 shows the design setup of the first proposed design. The proposed unit cell which is built on a substrate Rogers RT5880 that has a relative permittivity of 2.2, is characterized by dimensions $(7 \times 7 \times 0.8)\text{ mm}^3$. The simulation of the designed model was done through the use of CST. Table 1 below presents the design's dimensions.

Table 1. Dimensions of Figure 5.

Notation	Values/mm
L	7
L1	6
L2	4
L3	3

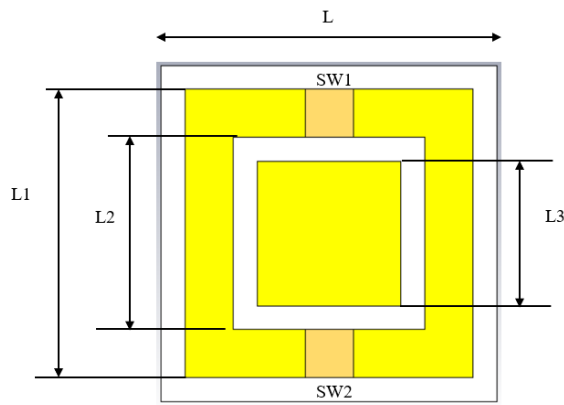


Figure 5. First proposed unit cell.

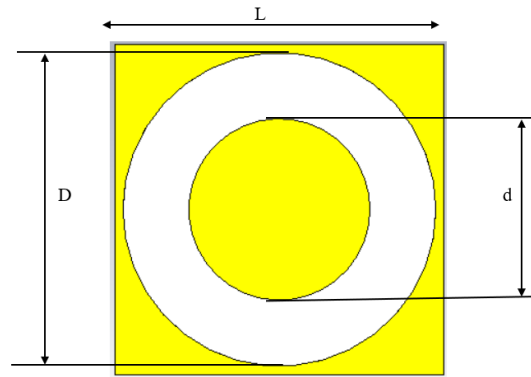


Figure 6. Second proposed unit cell.

Fig. 6 shows that the unit cells operate in a millimeter wave, and it is characterized by having a copper-coated top layer, excluding the circular split rings which are detached. The deployment of the unit cell is carried out on a Rogers RT5880 substrate with a relative permittivity of 2.2 and thickness of 0.8 mm. Meanwhile, the layer at the bottom is coated with copper. The entire measurement of the unit cell’s dimension is 6mm x 6mm x 0.8mm. The element parameters of the unit cell are depicted in mm in Table 2. Adjustments can be made to the phase and reflection coefficient of the design by changing the radius of the circular patch arbitrarily.

Table 2. Dimensions of Figure 6.

Notation	Values/mm
L	6
D	6
Patch diameter (d)	4

4. Results

With regards to the first proposed design which operates on the X-band, the phase and reflection coefficient are achieved through the selective changing of each state of the switch (on/off), with the switches exhibiting the behavior of the short and open circuit among the radiated patches. This first proposed design is equipped with four operation modes, with each of the four having its separate phase and reflection coefficient.

The GHz band coverage of the unit cell is (10-12). Details of the conditions of the pin diode at each operation mode as well as its phase and reflection coefficient are presented in Table 3. Also, the simulated Phase and Reflection Coefficient for the first proposed unit cell are presented in Fig.7 and 8.

Table 3. Pin diode conditions for different Phases and Reflection Coefficient.

Modes	Bands	SW1	SW2	Phase	Reflection Coefficient
1	11 GHz	OFF	OFF	-84.52	0.9896
2	11 GHz	OFF	ON	-177.48	0.9654
2	11 GHz	ON	OFF	-177.48	0.9654
3	11 GHz	ON	ON	82.804	0.97

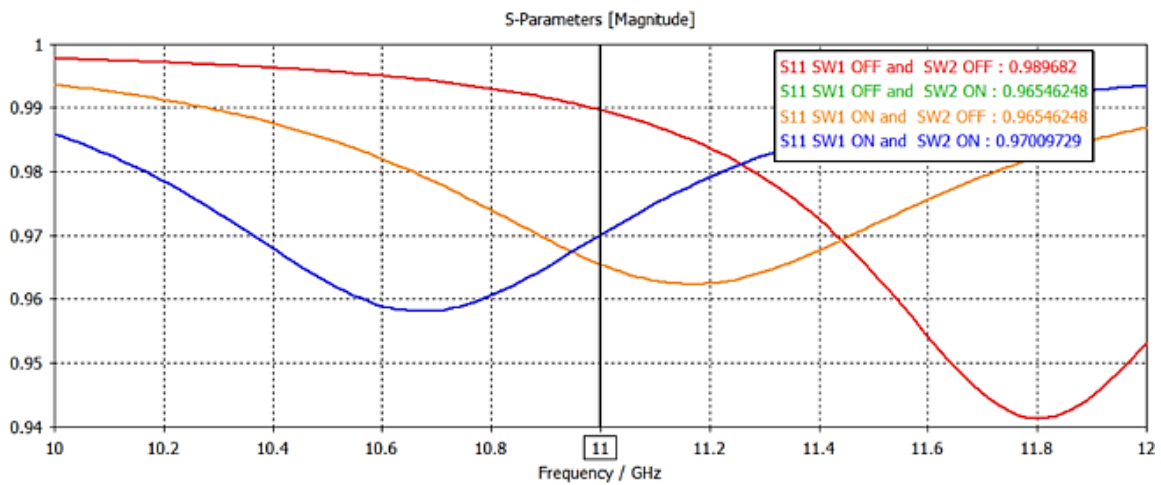


Figure 7. Reflection Coefficient of the first unit cell

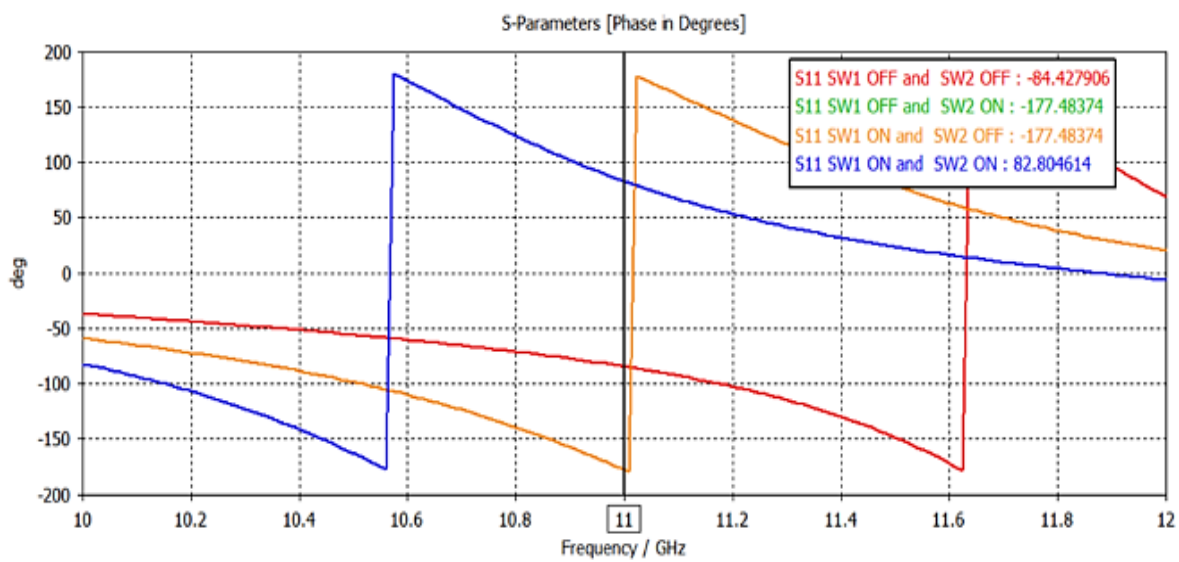


Figure 8. The phase of reflection for the first suggested unit cell.

In the second suggested design, the effect of using different patch radii is examined alongside the reflection Coefficient and phase properties showing that the unit cell serves as a reflector. between 25-32 GHz. Table 4 below

shows the Phase and Reflection Coefficient of the S11 parameters for the second proposed unit cell. The simulated phase as well as the reflection Coefficient of the unit cell are presented in Fig. 9 and 10.

Table 4. Different Phase and Reflection Coefficient due to change in patch radius

Modes	Bands	Radius	Phase	Reflection Coefficient
1	28 GHz	2.25	-131.21	0.997
2	28 GHz	1.4	135.09	0.996
3	28 GHz	1.65	61.371	0.987
4	28 GHz	1.8	-40.859	0.986

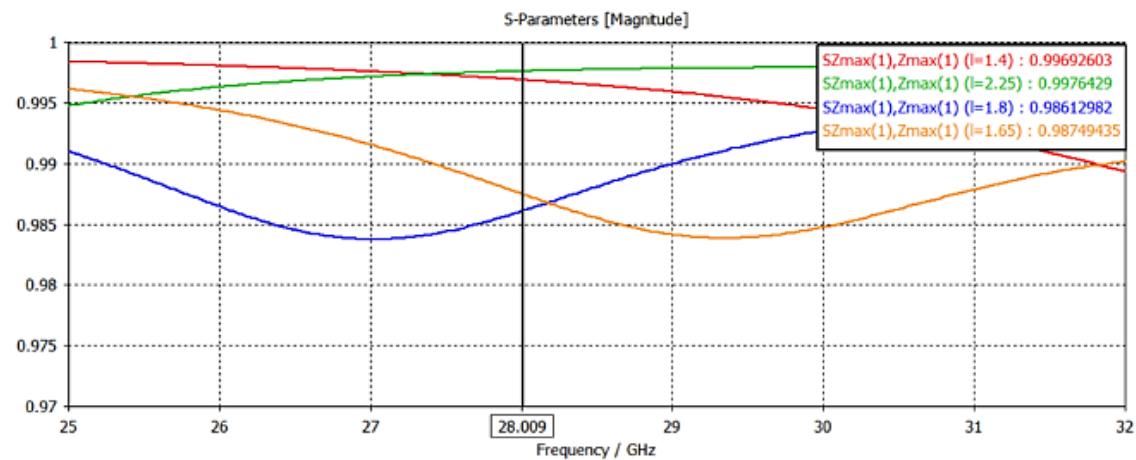


Figure 9. Reflection Coefficient of a second unit cell

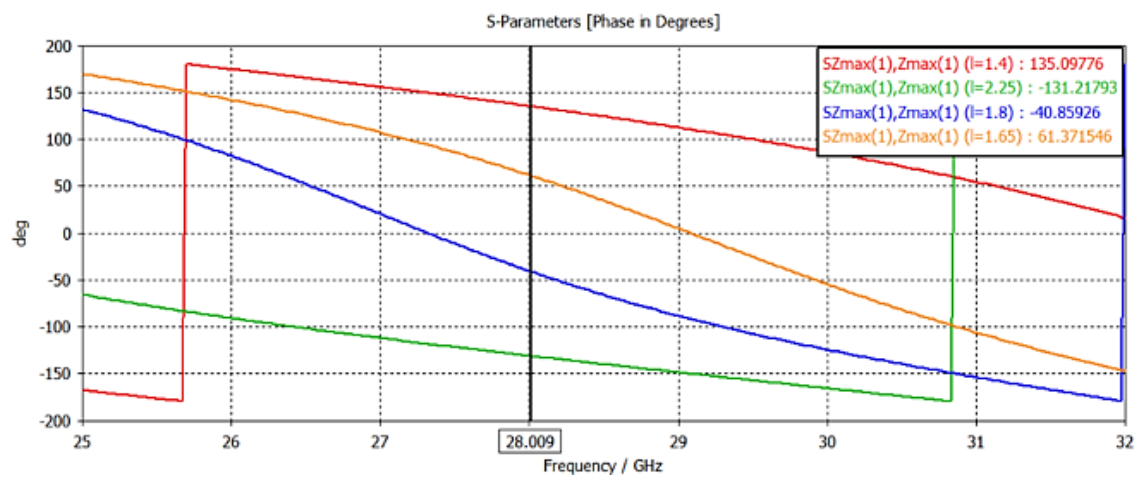


Figure 10. Reflection phase of the second unit cell

5. Conclusion

The unit cells proposed in this study have been simulated, and their performances have been presented in this article. The production of unit cells is quite easy due to their simplicity. In the RIS design of this study, the single-element unit cells were considered as the primary. Also, the adjustment of the phase and coefficient was done through the use of two techniques. The first technique involved tuning the state of the PIN diode, ON or OFF within the unit cell. In the second technique, the radius of the circular patch was changed. The reason for the selection of this kind of unit cell for the design of the RIS is the low cost of production as well as the ease with which it is constructed. One of the benefits that can be derived from the proposed design is its application in a wide range of reconfigurable systems including radar communication systems, satellite communication systems, and wireless communications because it is a low-profile and cost-effective design.

Acknowledgment

This work is supported by the College of Engineering/Mustansiriyah University, Iraq, Baghdad

Conflict of Interest

The authors confirm that publishing this paper does not produce any conflicting interests.

Author Contribution Statement

Jaafar Q. Kadhim formulated the theory and delineated the key concepts and evidence. Adheed H. Sallomi assisted in organizing and supervising this work. Jaafar Q. Kadhim implemented the experimental data, conducted the analysis using CST, and composed the manuscript. Adheed H. Sallomi provided assistance in analyzing the results and contributions made to the manuscript.

References

- [1] J. T. Kim and M. S. Todorovic, "Tuning control of buildings glazing's transmittance dependence on the solar radiation wavelength to optimize daylighting and building's energy efficiency," *Energy and Buildings*, vol. 63, pp. 108-118, 2013.
<https://doi.org/10.1016/j.enbuild.2013.03.036>
- [2] L. Levchenko et al., "Development of models of the electromagnetic environment in buildings and urbanized areas," *Eastern-European Journal of Enterprise Technologies*, vol. 6, no. 10, p. 120, 2022.
<https://doi.org/10.15587/1729-4061.2022.268439>
- [3] E. Basar, M. Di Renzo, J. De Rosny, M. Debbah, M.-S. Alouini, and R. Zhang, "Wireless communications through reconfigurable intelligent surfaces," *IEEE Access*, vol. 7, pp. 116753-116773, 2019.
<https://doi.org/10.1109/ACCESS.2019.2935192>
- [4] L. Dai et al., "Reconfigurable intelligent surface-based wireless communications: Antenna design, prototyping, and experimental results," *IEEE Access*, vol. 8, pp. 45913-45923, 2020. <https://doi.org/10.1109/ACCESS.2020.2977772>
- [5] R. Chen, M. Liu, Y. Hui, N. Cheng, and J. Li, "Reconfigurable intelligent surfaces for 6G IoT wireless positioning: A contemporary survey," *IEEE Internet of Things Journal*, vol. 9, no. 23, pp. 23570-23582, 2022. <https://doi.org/10.1109/JIOT.2022.3203890>
- [6] W. Long, R. Chen, M. Moretti, W. Zhang, and J. Li, "A promising technology for 6G wireless networks: Intelligent reflecting surface," *Journal of Communications and Information Networks*, vol. 6, no. 1, pp. 1-16, 2021. <https://doi.org/10.23919/JCIN.2021.9387701>
- [7] S. Zeng et al., "Reconfigurable intelligent surfaces in 6G: Reflective, transmissive, or both?" *IEEE Communications Letters*, vol. 25, no. 6, pp. 2063-2067, 2021. <https://doi.org/10.1109/LCOMM.2021.3062615>
- [8] T. Wang, G. Chen, M.-A. Badiu, and J. P. Coon, "Performance analysis of RIS-assisted large-scale wireless networks using stochastic geometry," *IEEE Transactions on Wireless Communications*, 2023. <https://doi.org/10.1109/TWC.2023.3250667>
- [9] T. L. Nguyen, T. N. Do, G. Kaddoum, D. B. da Costa, and Z. J. Haas, "Channel characterization for RIS-aided terahertz communications: A stochastic approach," *IEEE Wireless Communications Letters*, vol. 11, no. 9, pp. 1890-1894, 2022. <https://doi.org/10.1109/LWC.2022.3185977>
- [10] S. Guo, S. Lv, H. Zhang, J. Ye, and P. Zhang, "Reflecting modulation," *IEEE Journal on Selected Areas in Communications*, vol. 38, no. 11, pp. 2548-2561, 2020. <https://doi.org/10.1109/JSAC.2020.3007060>
- [11] S. P. Dash, R. K. Mallik, and N. Pandey, "Performance analysis of an index modulation-based receive diversity RIS-assisted wireless communication system," *IEEE Communications Letters*, vol. 26, no. 4, pp. 768-772, 2022. <https://doi.org/10.1109/LCOMM.2022.3147804>
- [12] E. Basar, "Reconfigurable intelligent surface-based index modulation: A new beyond MIMO paradigm for 6G," *IEEE Transactions on Communications*, vol. 68, no. 5, pp. 3187-3196, 2020.
<https://doi.org/10.1109/TCOMM.2020.2971486>
- [13] B. Li, Z. Zhang, Z. Hu, and Y. Chen, "Joint array diagnosis and channel estimation for RIS-aided mmWave MIMO system," *IEEE Access*, vol. 8, pp. 193992-194006, 2020. <https://doi.org/10.1109/ACCESS.2020.3032775>
- [14] J. He, H. Wymeersch, and M. Juntti, "Channel estimation for RIS-aided mmWave MIMO systems via atomic norm minimization," *IEEE Transactions on Wireless Communications*, vol. 20, no. 9, pp. 5786-5797, 2021. <https://doi.org/10.1109/TWC.2021.3070064>
- [15] B. C. Nguyen, T. M. Hoang, and T. Kim, "On performance of two-way full-duplex communication system with reconfigurable intelligent surface," *IEEE Access*, vol. 9, pp. 81274-81285, 2021. <https://doi.org/10.1109/ACCESS.2021.3086067>
- [16] Z. Yang et al., "Energy-efficient wireless communications with distributed reconfigurable intelligent surfaces," *IEEE Transactions on Wireless Communications*, vol. 21, no. 1, pp. 665-679, 2021. <https://doi.org/10.1109/TWC.2021.3098632>
- [17] Y. Zhang et al., "Beyond cell-free MIMO: Energy efficient reconfigurable intelligent surface aided cell-free MIMO communications," *IEEE Transactions on Cognitive Communications and Networking*, vol. 7, no. 2, pp. 412-426, 2021. <https://doi.org/10.1109/TCNN.2021.3058683>
- [18] M. Jian et al., "Reconfigurable intelligent surfaces for wireless communications: Overview of hardware designs, channel models, and estimation techniques," *Intelligent and Converged Networks*, vol. 3, no. 1, pp. 1-32, 2022. <https://doi.org/10.23919/ICN.2022.0005>
- [19] M. Ahmed et al., "A Survey on STAR-RIS: Use Cases, Recent Advances, and Future Research Challenges," *IEEE Internet of Things Journal*, 2023. <https://doi.org/10.1109/JIOT.2023.3279357>
- [20] E. C. Strinati et al., "Reconfigurable, intelligent, and sustainable wireless environments for 6G smart connectivity," *IEEE Communications Magazine*, vol. 59, no. 10, pp. 99-105, 2021. <https://doi.org/10.1109/MCOM.001.2100070>
- [21] A. Shahraki, M. Abbasi, M. J. Piran, and A. Taherkordi, "A comprehensive survey on 6G networks: Applications, core services, enabling technologies, and future challenges," *arXiv preprint arXiv:2101.12475*, 2021. <https://doi.org/10.48550/arXiv.2101.12475>
- [22] X. Cheng et al., "Joint optimization for RIS-assisted wireless communications: From physical and electromagnetic perspectives," *IEEE Transactions on Communications*, vol. 70, no. 1, pp. 606-620, 2021. <https://doi.org/10.1109/TCOMM.2021.3120721>
- [23] Y. Liu et al., "Reconfigurable intelligent surfaces: Principles and opportunities," *IEEE Communications Surveys & Tutorials*, vol. 23, no. 3, pp. 1546-1577, 2021. <https://doi.org/10.1109/COMST.2021.3077737>
- [24] C. Pan et al., "An overview of signal processing techniques for RIS/IRS-aided wireless systems," *IEEE Journal of Selected Topics in Signal Processing*, 2022. <https://doi.org/10.1109/JSTSP.2022.3195671>
- [25] K. Sarabandi, M. D. Casciato, and I.-S. Koh, "Efficient calculation of the fields of a dipole radiating above an impedance surface," *IEEE Transactions on Antennas and Propagation*, vol. 50, no. 9, pp. 1222-1235, 2002. <https://doi.org/10.1109/TAP.2002.7054733>
- [26] S. Gharbieh, R. D'Errico, and A. Clemente, "Reconfigurable Intelligent Surface Design using PIN Diodes via Rotation Technique—Proof of Concept," in *2023 17th European Conference on Antennas and Propagation (EuCAP)*, 2023: IEEE, pp. 1-4. <https://doi.org/10.23919/EuCAP57121.2023.10133091>
- [27] P.-Y. Qin, A. R. Weily, Y. J. Guo, and C.-H. Liang, "Polarization reconfigurable U-slot patch antenna," *IEEE Transactions on Antennas and Propagation*, vol. 58, no. 10, pp. 3383-3388, 2010. <https://doi.org/10.1109/LAWP.2023.3309504>
- [28] L. G. da Silva, Z. Chu, P. Xiao, and A. Cerqueira S Jr, "A varactor-based 1024-element RIS design for mm-waves," *Frontiers in Communications and Networks*, vol. 4, p. 1086011, 2023. <https://doi.org/10.3389/frcmn.2023.1086011>
- [29] C. Liu, F. Yang, S. Xu, and M. Li, "A novel design method of RIS element with a wideband varactor-tuned example," in *2023 IEEE International Symposium on Antennas and Propagation and USNC-URSI Radio Science Meeting (USNC-URSI)*, 2023: IEEE, pp. 975-976. <https://doi.org/10.1109/USNCURSI52151.2023.10237724>

- [30] M. G. Silveirinha, C. A. Fernandes, and J. R. Costa, "Electromagnetic characterization of textured surfaces formed by metallic pins," *IEEE Transactions on Antennas and Propagation*, vol. 56, no. 2, pp. 405-415, 2008. <https://doi.org/10.1109/TAP.2007.915442>
- [31] A. Araghi et al., "Reconfigurable intelligent surface (RIS) in the sub-6 GHz band: Design, implementation, and real-world demonstration," *IEEE Access*, vol. 10, pp. 2646-2655, 2022. <https://doi.org/10.1109/ACCESS.2022.3140278>
- [32] X. Pei et al., "RIS-aided wireless communications: Prototyping, adaptive beamforming, and indoor/outdoor field trials," *IEEE Transactions on Communications*, vol. 69, no. 12, pp. 8627-8640, 2021. <https://doi.org/10.1109/TCOMM.2021.3116151>
- [33] L. G. da Silva, P. Xiao, and A. Cerqueira, "A 2-bit tunable unit cell for 6G reconfigurable intelligent surface application," in *2022 16th European Conference on Antennas and Propagation (EuCAP)*, 2022: IEEE, pp. 1-5. <https://doi.org/10.23919/EuCAP53622.2022.9769482>
- [34] J.-B. Gros, V. Popov, M. A. Odit, V. Lenets, and G. Lerosey, "A reconfigurable intelligent surface at mmWave based on a binary phase tunable metasurface," *IEEE Open Journal of the Communications Society*, vol. 2, pp. 1055-1064, 2021. <https://doi.org/10.1109/OJCOMS.2021.3076271>
- [35] Q. Hu et al., "Design of a novel 2-bit wideband beam-scanning reconfigurable intelligent surface," in *2021 IEEE International Workshop on Electromagnetics: Applications and Student Innovation Competition (iWEM)*, 2021: IEEE, pp. 1-3. <https://doi.org/10.1109/iWEM53379.2021.9790574>
- [36] G. C. Trichopoulos et al., "Design and evaluation of reconfigurable intelligent surfaces in real-world environment," *IEEE Open Journal of the Communications Society*, vol. 3, pp. 462-474, 2022. <https://doi.org/10.1109/OJCOMS.2022.3158310>
- [37] X. Zeng et al., "High-accuracy reconfigurable intelligent surface using independently controllable methods," in *2021 IEEE International Workshop on Electromagnetics: Applications and Student Innovation Competition (iWEM)*, 2021: IEEE, pp. 1-3. <https://doi.org/10.1109/iWEM53379.2021.9790555>
- [38] J. Rains, L. Zhang, Q. H. Abbasi, M. Imran, and A. Tukmanov, "2.75-bit reflecting unit cell design for reconfigurable intelligent surfaces," in *2021 IEEE International Symposium on Antennas and Propagation and USNC-URSI Radio Science Meeting (APS/URSI)*, 2021: IEEE, pp. 335-336. <https://doi.org/10.1109/APS/URSI47566.2021.9704689>
- [39] S. Zhao, R. Langwieser, and C. F. Mecklenbraeuer, "Reconfigurable digital metasurface for 3-bit phase encoding," in *WSA 2021; 25th International ITG Workshop on Smart Antennas*, 2021: VDE, pp. 1-6. https://publik.tuwien.ac.at/files/publik_296864.pdf
- [40] J. Rains, A. Tukmanov, T. J. Cui, L. Zhang, Q. H. Abbasi, and M. A. Imran, "High-resolution programmable scattering for wireless coverage enhancement: an indoor field trial campaign," *IEEE Transactions on Antennas and Propagation*, vol. 71, no. 1, pp. 518-530, 2022. <https://doi.org/10.1109/TAP.2022.3216555>
- [41] A. H. Sallomi, "Enabling Deep Learning and Swarm Optimization Algorithm for Channel Estimation for Low Power RIS Assisted Wireless Communications," *International Journal of Interactive Mobile Technologies*, vol. 17, no. 12, 2023. <https://doi.org/10.3991/ijim.v17i12.39411>
- [42] J. Q. Kadhim and A. H. Sallomi, "Systematic review of the reconfigurable intelligent surfaces through wireless communication," in *AIP Conference Proceedings*, 2023, vol. 2977, no. 1: AIP Publishing. <https://doi.org/10.1063/5.0182238>
- [43] J. Q. Kadhim, "Design and Implementation Unit Cell for 6G Reconfigurable Intelligent Surface Application," *International Journal of Online & Biomedical Engineering*, vol. 19, no. 5, 2023. <https://doi.org/10.3991/ijoe.v19i05.37585>
- [44] B. Rana, S.-S. Cho, and I.-P. Hong, "Parameters and measurement techniques of reconfigurable intelligent surfaces," *Micromachines*, vol. 13, no. 11, p. 1841, 2022. <https://doi.org/10.3390/mi13111841>
- [45] R. B. Nassir and A. K. Jassim, "Design of mimo antenna for wireless communication applications," *Journal of Engineering and Sustainable Development (JEASD)*, vol. 26, no. 4, 2022. <https://doi.org/10.31272/jeasd.26.4.4>
- [46] A. K. Nghaimesh and A. K. Jassim, "Triple-Band Circular Patch Microstrip Antenna for Wireless Communication," *Journal of Engineering and Sustainable Development*, vol. 28, no. 1, pp. 64-74, 2024. <https://doi.org/10.31272/jeasd.28.1.5>
- [47] S. K. Hassan, and M. H. Wali, "DESIGN OF A DUAL-BAND REJECTION PLANAR ULTRA-WIDEBAND (UWB) ANTENNA," *Journal of Engineering and Sustainable Development*, vol. 26, no. 4, pp. 30-35, 2022. <https://doi.org/10.31272/jeasd.26.4.3>
- [48] N. A. Jazea, and H. A. Kadim, "Study and analysis of intra-cell interference and inter-cell interference for 5G network," *Journal of Engineering and Sustainable Development*, vol. 24, no. 3, pp. 43-57, 2020. <https://doi.org/10.31272/jeasd.24.3.3>